Gait Entrainment to Torque Pulses From a Hip Exoskeleton Robot

Jongwoo Lee, *Student Member, IEEE*, Meghan E. Huber, *Member, IEEE*, and Neville Hogan, *Member, IEEE*

***Abstract*— Robot-aided locomotor rehabilitation has proven challenging. To facilitate progress, it is important to first understand the neuro-mechanical dynamics and control of unimpaired human locomotion. Our previous studies found that human gait entrained to periodic torque pulses at the ankle when the pulse period was close to preferred stride duration. Moreover, synchronized gait exhibited a constant phase relation with the pulses so that the robot provided mechanical assistance. To test the generality of mechanical gait entrainment, this study characterized unimpaired human subjects' responses to periodic torque pulses during overground walking. The intervention was applied by a hip exoskeleton robot, Samsung GEMS-H. Gait entrainment was assessed based on the time-course of the phase at which torque pulses occurred within each stride. Experiments were conducted for two consecutive days to evaluate whether the second day elicited more entrainment. Whether entrainment was affected by the difference between pulse period and preferred stride duration was also assessed. Results indicated that the intervention evoked gait entrainment that occurred more often when the period of perturbation was closer to subjects' preferred stride duration, but the difference between consecutive days was insignificant. Entrainment was accompanied by convergence of pulse phase to a similar value across all conditions, where the robot maximized mechanical assistance. Clear evidence of motor adaptation indicated the potential of the intervention for rehabilitation. This study quantified important aspects of the nonlinear neuro-mechanical dynamics underlying unimpaired human walking, which will inform the development of effective approaches to robot-aided locomotor rehabilitation, exploiting natural dynamics in a minimally-encumbering way.**

***Index Terms*— Hip exoskeleton robot, gait entrainment, locomotor rehabilitation.**

Manuscript received September 20, 2021; revised January 14, 2022; accepted February 9, 2022. Date of publication March 14, 2022; date of current version March 22, 2022. This work was supported in part by the Global Research Outreach Program of Samsung Advanced Institute of Technology and in part by the Eric P. and Evelyn E. Newman Fund. Jongwoo Lee was supported in part by a Samsung Scholarship. *(Corresponding author: Jongwoo Lee.)*

Jongwoo Lee was with the Department of Mechanical Engineering, Massachusetts Institute of Technology, Cambridge, MA 02139 USA (e-mail: jw127@mit.edu).

Meghan E. Huber is with the Department of Mechanical and Industrial Engineering, University of Massachusetts Amherst, Amherst, MA 01003 USA (e-mail: mehuber@umass.edu).

Neville Hogan is with the Department of Mechanical Engineering and the Department of Brain and Cognitive Sciences, Massachusetts Institute of Technology, Cambridge, MA 02139 USA (e-mail: neville@mit.edu).

Digital Object Identifier 10.1109/TNSRE.2022.3155770

I. Introduction

THE incidence of gait and balance disorders is expected to rise with the aging of the population and consequent increase in neurological injuries and disorders such as stroke [1]–[4]. Thus, there is a great need for effective methods to aid and restore human locomotion.

Robot-aided locomotor therapy has emerged as a promising method to meet the enormous demand, as it allows repetitive, high-intensity, and task-oriented training in a safe and efficient manner [5], which is important for successful rehabilitation. There is evidence to suggest that complementing conventional gait therapy with robot-aided training can be beneficial [6]. But on its own, robot-aided gait therapy does not outperform conventional physical therapy in clinical measures (such as walking speed, step length, and step frequency) [7]. The recent rise of autonomously powered exoskeleton robots promises new avenues for delivering therapy in more ecological contexts, outside of a formal clinical setting [8]–[10]. However, to live up to their promise and maximize gait recovery, we must better understand natural human locomotion and how humans react to exoskeletal robotic interventions.

Earlier robotic gait rehabilitation approaches have been criticized as they enforced repetition of preprogrammed kinematics which may have discouraged active engagement of participants and suppressed the natural rhythmic dynamics of walking [7], [11], [12]. Our previous studies proposed a novel robotic intervention to modulate gait frequency—gait entrainment—that respects the rhythmic dynamic nature of walking [13]. It was shown that applying periodic torque pulses at the ankle, using an ankle exoskeleton robot, could induce subjects to increase their cadence to synchronize with the period of the pulses, when the pulse period was close to but shorter than subjects' preferred stride duration. This experimental observation suggests that a nonlinear neuro-mechanical limit cycle oscillator is a reasonable description of the dynamics of human walking. Moreover, subjects adapted their gait so that plantar-flexion torque pulses from the robot aligned with ankle push-off, which maximized their mechanical assistance. Subsequent studies showed that entrainment was observed more often, occurred earlier, and persisted longer during overground walking compared to treadmill walking [11]. Motivated by this success with healthy individuals, Ahn *et al.* studied the feasibility of this intervention to treat locomotor deficits of neurologically-impaired patients and increase their cadence and walking speed [14].

This paradigm is similar to auditory entrainment but different in that it involves physical interaction and energy exchange. Gait entrainment to rhythmic, auditory signals is well-known and has been studied in depth [15]–[18], but synchronization to other forms of rhythmic stimuli is underexplored. Since the pioneering work of Ahn and Hogan that investigated gait entrainment to exoskeletal mechanical signals [13], there is a growing interest in gait entrainment to various types of stimuli, including an oscillating treadmill [19], [20], periodic vertical force [21], and electrical muscle stimulation [22], [23]. These studies share the motivation that gait entrainment holds promise for locomotor rehabilitation, as well as providing a useful experimental paradigm to better inform neuro-motor control of human walking. However, results also show that while promising, gait entrainment is not straightforward to achieve.

The goal of the present study was to test whether humans also entrain to periodic torque pulses applied at the hip joints while walking overground. Torque pulses were applied by an autonomous hip exoskeleton robot, the Samsung Gait Enhancing and Motivating Systems for Hip (GEMS-H). We hypothesized that subjects would entrain their gait to periodic perturbations applied to the hip joint, consistent with prior results from ankle entrainment studies. A preliminary study showed that entrainment to hip torque pulses seemed promising [24]. In the study reported here, experiments were conducted for two consecutive days to evaluate whether the second day elicited more entrainment. We also assessed how increasing the difference between the torque pulse period and subjects' preferred stride duration affected human responses. Assessment of gait entrainment requires accurate and reliable phase estimation. We developed an off-line stride segmentation algorithm and applied a phase estimation algorithm developed in [25], which does not require external sensors such as motion capture or foot-switches. Finally, we investigated whether subjects aligned the torque pulses to a specific phase of the gait cycle; and whether it was related to the mechanical power or work done by the hip exoskeleton robot, similar to the behavior observed in prior entrainment studies using an ankle exoskeleton [11], [26].

II. Methods

A. Subjects

A total of fifteen healthy young adults (gender: 4 females, 11 males; mean age: 25.5 ± 5.1 years old) participated in this study. The total number of subjects was chosen to be slightly larger than that which yielded statistically significant results in a related prior study of entrainment to periodic ankle torques [11]. Subjects were divided into two groups: group-25ms ($N = 7$) and group-50ms ($N = 8$). All subjects gave informed written consent before the experiment. The experimental protocol was reviewed and approved by the Institutional Review Board of the Massachusetts Institute of Technology (protocol #: 1809534122; approval date: 10/18/2018).

B. Equipment: Samsung GEMS-H Exoskeleton

The Samsung Gait Enhancing and Motivating Systems for Hip (GEMS-H) developed by Samsung Advanced Institute of Technology (Suwon, South Korea) was used in this study (Fig. 1A; [27]–[30]). This low-mass (2.1 kg) robot is worn around the waist and fastened to the thighs. A pair of actuators, one at each hip joint, applies torque in the sagittal plane (hip flexion and extension). Passive hinges allow unencumbered hip ab/adduction motion in the frontal plane. The torque output of each actuator is estimated and controlled by sensing electrical current in the respective motor. Encoders embedded in the actuator modules measure hip joint angles. All electronics, actuators, and power sources are located onboard the device, allowing for untethered operation. Unlike laboratory-based tethered exoskeleton testbeds [31]–[34], this autonomous exoskeleton allows experiments to be conducted overground, thereby enabling study of the effects of intervention in more ecological contexts.

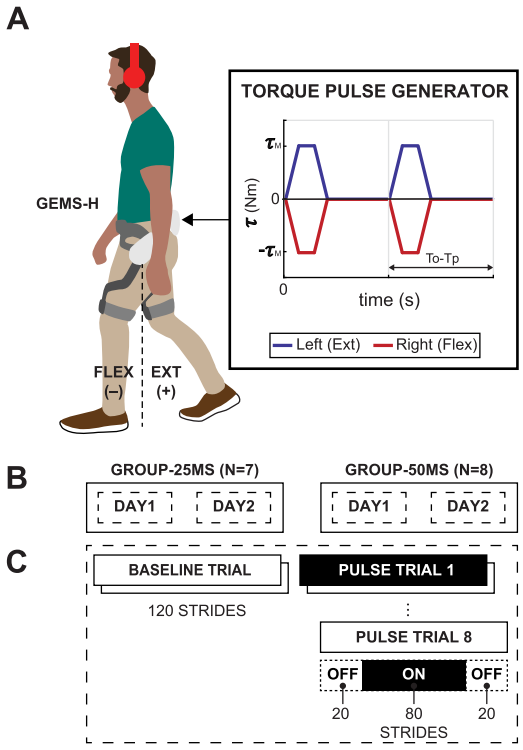

Fig. 1. **A** The Samsung GEMS-H exoskeleton applied torque pulses between the two thighs. Subjects were instructed to walk comfortably. **B** Subjects were divided into two groups. **C** Experimental protocol for each day.

C. Experimental Procedure

On two consecutive days, all subjects performed ten walking trials (two baseline trials followed by eight pulse trials) per day wearing the GEMS-H exoskeleton (Fig. 1A). Each trial consisted of 120 strides, and all trials were performed in a long corridor (approximately 250 m) with low foot traffic to simulate real-world walking conditions. Throughout the trials, subjects listened to white noise through wireless, over-the-ear headphones to mask the sound of the exoskeleton and environment. Subjects were instructed to walk at their comfortable pace, but they were neither informed that the torque

pulses would be delivered periodically, nor asked to "entrain" to these perturbations. The experiment lasted approximately 45 minutes on each day.

1) Baseline Trials: In baseline trials, the hip exoskeleton was unpowered (i.e., zero motor current), and subjects were instructed to walk at a comfortable pace. On each day, preferred stride duration (T_o) was quantified as the average stride period from the middle 30 strides in the second baseline trial.

2) Pulse Trials: In the pulse trials, the hip exoskeleton was unpowered during the first 20 strides, powered during the subsequent 80 strides, and unpowered for the remaining 20 strides (Fig. 1B). When powered, the exoskeleton delivered periodic torque pulses to both legs simultaneously. The torque pulses were trapezoidal in shape with a duration (T_d) of 200 ms (Fig. 1A). The magnitude of peak torque (τ_M) was set to 0.1 times the subject's body mass in kg and was constant across trials for each subject. For safety, the torque magnitude was upper bounded by 8 Nm (group-25ms: median = 7.2 Nm, inter-quartile range (IQR) = 1.2 Nm; group-50ms: median = 8 Nm, IQR = 1.4 Nm). Note that the magnitude of torque applied was only ∼10% of the magnitude of the peak hip moment during natural gait [35].

The torque pulse applied to the right hip (τ_R) was always in the flexion direction (negative) and in the extension direction (positive) for the left hip (τ_L). The torques to the left and right hips were always of the same magnitude but opposite direction, i.e., $\tau_R + \tau_L = 0$ (Fig. 1A). For subjects in group-25ms, the pulse period (T_p) was set to be 25 ms faster than their preferred stride duration ($T_o - T_p = 25$ ms); for subjects in group-50ms, the pulse period was set to be 50 ms faster than their preferred stride duration ($T_o - T_p = 50$ ms). Subjects were instructed to walk in whatever way they found most comfortable. They were aware that the exoskeleton would alternate between powered and unpowered states during these trials, but they were not informed how the exoskeleton was controlled.

D. Hypotheses

To understand whether a nonlinear stable limit cycle oscillator is a reasonably competent descriptive model of the neuro-mechanical system controlling human walking, we assessed how the difference between torque pulse period and subjects' preferred stride duration affected entrainment. We hypothesized that entrainment would be observed more often when the difference was smaller, i.e., more often in group-25ms than in group-50ms (**hypothesis 1**). Synchronization itself does not specify the phase at which entrainment occurs. However, if entrainment occurs due to the dynamic structure of the human walking controller, a consistent phase when entrained was expected. Therefore, we hypothesized that the phase when entrained would be consistent across trials and subjects, i.e., for all entrained trials the distributions of the terminal pulse phases would not be different (**hypothesis 2**).

It is important to assess neural and/or biomechanical contributions. Experiments were conducted for two consecutive days to evaluate whether the second day elicited more entrainment. If the central nervous system (CNS) learned the adapted behavior, repeated bouts should evoke more frequent entrainment. We hypothesized that entrainment would be observed more often on day 2 than on day 1 (**hypothesis 3**). Lastly, we tested whether mechanical energy/work done by the robot had any relation to entrainment, similar to the behavior observed in the prior entrainment studies using an ankle exoskeleton. We hypothesized that the locking phase would be commensurate with the phase where the torque pulse could provide maximal positive power (**hypothesis 4**).

E. Data Processing

1) Stride Segmentation: Each stride began with maximum extension (positive) of the left hip angle (θ_L), which approximately corresponds to left toe-off [36]. Because torque pulses applied during the pulse trials affected position measurements, simple peak detection did not reliably separate each stride from the entire time-series data. To account for the inevitable relative motion between the exoskeleton and the wearer, we developed an off-line stride segmentation algorithm, as described in Appendix **I**.

2) Phase Estimation: Determining phase variables from experimental signals is not trivial, especially when the signals are non-stationary [37], [38]. Previous studies [39], [40] proposed to compute phase from kinematic observations (kinematic phase) to understand neuromechanical control of animal locomotion subject to mechanical perturbation. Recent work in the robotics community exploited kinematic phase variables to design biped walking controllers, and this showed more robust performance than using a time-based phase variable [41]. Inspired by these previous studies, Gregg and colleagues [25], [42]–[44] recently proposed reliable and robust methods to determine a phase variable for human walking, using hip angle. We adopted this method to estimate the gait phase of human subjects ϕ from the angular positions measured from the exoskeleton encoder of the left hip joint (θ_L). The estimated phase was used to assess entrainment, and to investigate to which phase of the gait cycle the mechanical perturbations converged. We briefly present the method in Appendix II, but readers are referred to the original work for details.

F. Dependent Measures

1) Pulse Phase: Pulse phase ϕ_P (%) was defined as the phase at which the onset of the torque pulse occurred within the gait cycle. The initial pulse phase ($\phi_{P,initial}$) of a given trial refers to the pulse phase of the first pulse and the terminal pulse phase ($\phi_{P,terminal}$) refers to average pulse phase of the last 10 pulses in that trial.

2) Pulse Phase Slope: Pulse phase slope (%/#) was defined as the average change of pulse phase (%) with respect to pulse number (#). Pulse phase slope was computed over the first 10 pulses (*initial pulse phase slope*) and the last 10 pulses (*terminal pulse phase slope*) of each trial by linear regression (MATLAB function `fitlm`).

3) Entrainment Criteria: Each trial was classified as *entrained* if the magnitude of the terminal pulse phase slope was < 0.5 (%/#); otherwise, it was classified as *not-entrained*.

4) Period Deviation: Period deviation ΔT (ms) was defined as the difference between each stride duration and the torque pulse period for each respective trial.

5) Pulse Mechanical Energy: Normalized pulse mechanical energy E_P (J/Nm) passed from the robot to the human was estimated for each torque pulse by integrating instantaneous power over time. To normalize the measure, the net energy was divided by peak commanded torque (τ_M) of the corresponding trial $E_p \approx \frac{1}{\tau_M}\int \left(\tau_R \dot{\theta}_R + \tau_L \dot{\theta}_L\right) dt$. The joint torques were estimated from the current sensors. Joint position signals were filtered to estimate joint velocities off-line using an FIR filter (order: 50, passband: 20 Hz, stopband: 30 Hz) to approximate an ideal low-pass filtered differentiator. The group delay of the filter was used to compensate for the time shift of the signals due to the filtering process. Signal processing was performed using MATLAB R2018b (Mathworks, MA; function: `designfilt`).

6) Predicted Pulse Phase: Ignoring kinematic variation induced by the robot perturbation, one can estimate the dependence of pulse mechanical energy on pulse phase. Assuming an ideal pulse was applied to the wearers with magnitude $\tau_M (= \tau_L = -\tau_R)$, and using the kinematics obtained during baseline trials, the estimated pulse mechanical energy was calculated as

$$\hat{E}_P(\phi_P) \approx \frac{1}{\tau_M}\int \tau_M(\dot{\theta}_L - \dot{\theta}_R)dt = \Delta\theta_{REL}(\phi_P), \qquad (1)$$

where $\theta_{REL} = \theta_L - \theta_R$, $\Delta\theta_{REL} = \theta_{REL}(t_{on}(\phi_P) + T_d) - \theta_{REL}(t_{on}(\phi_P))$, and t_{on} is the pulse onset time corresponding to ϕ_P. Based on **hypothesis 4**, we predicted the pulse phase $\hat{\phi}_P$ (%) would maximize the pulse mechanical energy, i.e. $\hat{\phi}_P = \text{argmax}_{\phi_P} \hat{E}_P(\phi_P)$.

G. Statistical Analyses

Statistical analyses were conducted using the Statistics and Machine Learning Toolbox of MATLAB R2018b (Mathworks, MA). For all statistical tests, the significance level was set to $\alpha = 0.05$. For each analysis of variance (ANOVA), the F-statistic and corresponding p-value are reported for all main effects and interactions.

A 2 (group: 25ms vs. 50ms) × 2 (day: 1 vs 2) ANOVA on the number of entrained trials was performed to test whether entrainment occurred more often when the difference between natural stride duration and pulse period was smaller (**hypothesis 1**) and whether the second day elicited more entrainment (**hypothesis 3**). Group was a between-subjects factor and day was a within-subject factor.

A 2 (group: 25ms vs. 50ms) × 2 (day: 1 vs. 2) ANOVA on terminal pulse phase ($\phi_{P,terminal}$) of entrained trials tested whether the terminal pulse phase (i.e., locking phase) was influenced by the experimental conditions (**hypothesis 2**). Group was a between-subjects factor and day was a within-subject factor.

A residual analysis was conducted to compare the agreement between the actual pulse phase and predicted pulse phase for maximizing mechanical work $\hat{\phi}_P$ (%) during the last ten pulses of each trial (**hypothesis 4**).

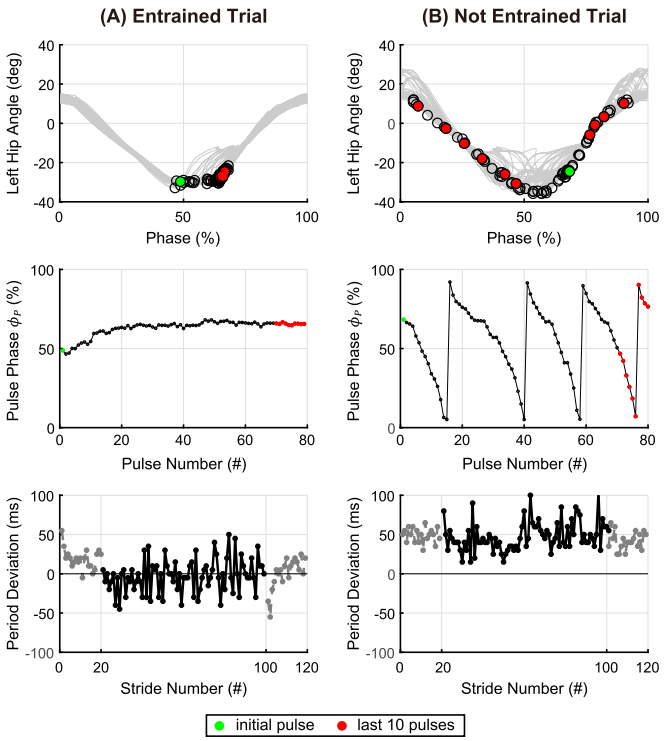

Fig. 2. **A** Representative entrained trial. **B** Representative not-entrained trial. Top: Left hip angle vs. phase, all strides. Black circles denote onsets of torque pulses. Middle: Pulse phase (ϕ_P) vs. pulse number. Bottom: Period deviation vs. stride number. Torque pulses were applied during strides 20-100 (black, solid). Pre- and post-pulse strides are also plotted (gray, dotted). In the top and middle rows, the initial pulse (green dot) and the last 10 pulses (red dots) are highlighted.

III. Results

A. Representative Trials

Fig. 2 presents two representative trials: entrained (group-25ms, day 1, subject 1, trial 1) and not-entrained (group-50ms, day 1, subject 2, trial 1). In the entrained trial (Fig. 2A), the pulse phase converged by the end of the trial (M: 65.6%, SD: 0.54% in the last 10 pulse phases). The stride duration was approximately matched to the torque pulse period (i.e., period deviation close to zero). After the torque pulses ceased, stride duration slowly returned towards its pre-perturbation value (stride number 100 - 120). However, in the not-entrained trial (Fig. 2B), the pulse phase drifted through all phases of the gait cycle and stride duration was little affected by the intervention (non-zero period deviation).

B. Group Results

Consistent with **hypothesis 1**, gait entrainment was observed more frequently in group-25ms (day1: 71%, 40 out of 56 trials; day2: 79%, 44 out of 56 trials) than in group-50ms (day1: 39%, 25 out of 64 trials; day2: 45%, 29 out of 64 trials), and this difference was statistically significant ($F[1, 13] = 7.8, p = 0.015$). Counter to **hypothesis 3**, there was no statistical difference between consecutive days of experiments ($F[1, 13] = 0.37, p = 0.55$). There was no statistically significant interaction between groups and

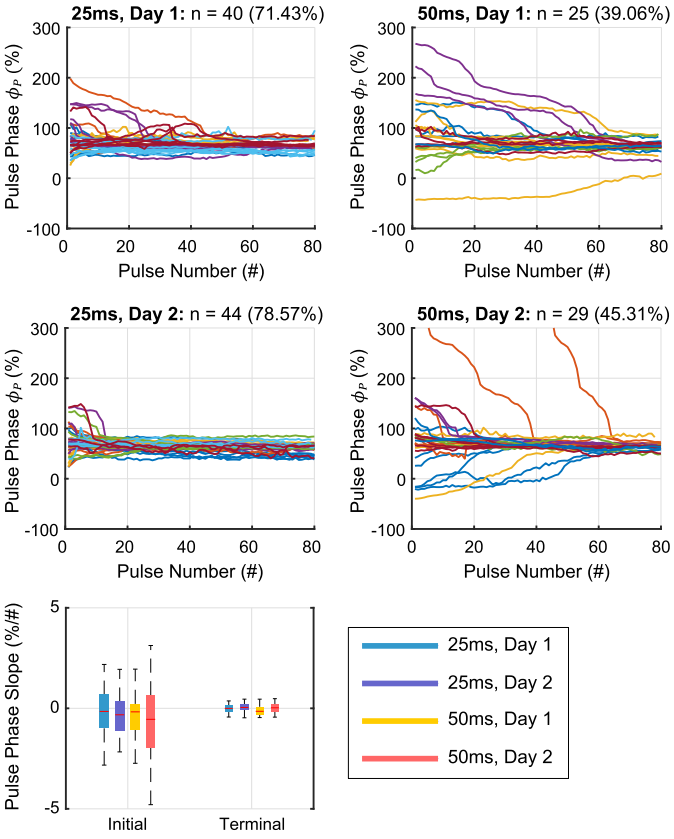

Fig. 3. Pulse phase (ϕ_P) vs. pulse number for all entrained trials in all conditions. The number (n) of entrained trials, along with the percentage of entrained trials, for each condition is also presented. Different colors represent different subjects. The pulse phases are unwrapped such that the last value of each trial is between 0 % and 100 %. Pulse phase slope of initial and terminal segments of the entrained trials are also presented.

TABLE I
PERCENTAGE OF ENTRAINED TRIALS PER SUBJECT

	Subject	Day1 (%)	Day2 (%)	Total (%)
25ms	1	87.50	87.50	87.50
	2	75.00	100.00	87.50
	3	62.50	87.50	75.00
	4	87.50	100.00	93.75
	5	0.00	62.50	31.25
	6	100.00	75.00	87.50
	7	87.50	37.50	62.50
50ms	8	50.00	75.00	62.50
	9	0.00	100.00	50.00
	10	100.00	37.50	68.75
	11	37.50	25.00	31.25
	12	50.00	25.00	37.50
	13	0.00	0.00	0.00
	14	50.00	75.00	62.50
	15	25.00	25.00	25.00

days ($F[1, 13] = 0.002$, $p = 0.97$). The percentages of the entrained trials for individual subjects are listed in Table I.

Fig. 3 presents the progression of pulse phase (ϕ_P) vs. pulse number for all entrained trials for each condition. In entrained trials, pulse phase converged to an approximately constant value before the perturbation ceased. Within each trial, the pulse phases tended to drift in one direction (either increasing or decreasing). Fig. 3 (bottom) presents the distribution of the initial pulse phase slopes and the terminal pulse phase slopes

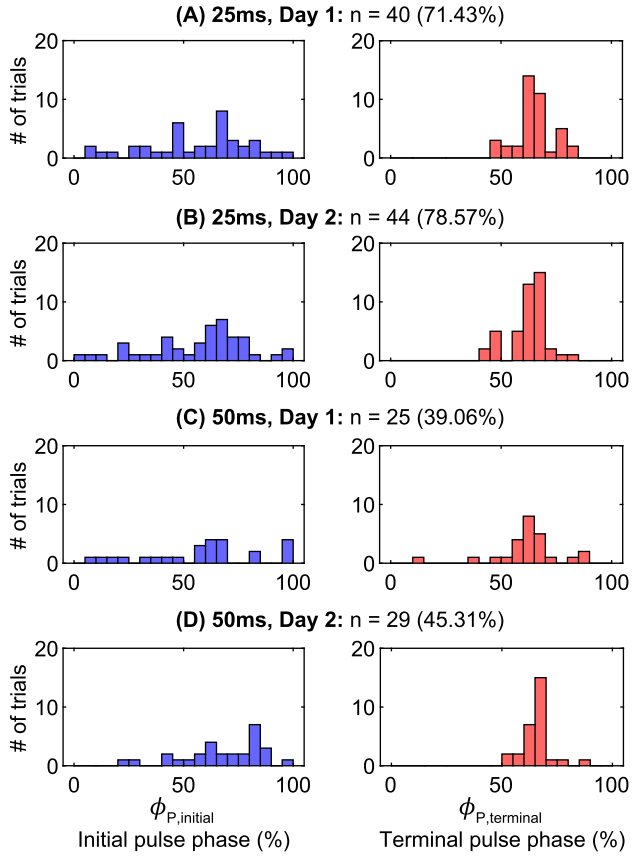

Fig. 4. Histograms of initial and terminal pulse phases ($\phi_{P,initial}$ and $\phi_{P,terminal}$, respectively) for all entrained trials across all conditions.

of the entrained trials. After initial transients, subjects adapted their gait and reached steady-state motion within 80 strides.

C. Gait Phase Convergence

Fig. 4 presents initial and terminal pulse phases ($\phi_{P,initial}$ and $\phi_{P,terminal}$, respectively) of the entrained trials across all conditions. While the $\phi_{P,initial}$ values were distributed widely across the entire gait cycle, the $\phi_{P,terminal}$ values formed a unimodal distribution in each condition. Consistent with **hypothesis 2**, $\phi_{P,terminal}$ was consistent across all entrained trials (M = 63.8 %); neither the effect of period difference (group-25ms vs. group-50ms; $F[1, 137] = 0.001$, $p = 0.97$), day (day1 vs. day2: $F[1, 137] = 0.08$, $p = 0.78$), nor their interaction ($F[1, 137] = 2.96$, $p = 0.088$) were statistically significant.

D. Mechanical Energy

Fig. 5 compares the normalized pulse mechanical energy E_P and ϕ_P values from the last 10 pulses of entrained and not-entrained trials in all conditions. The histograms of the entrained trials show that these two quantities were closely related. The unimodal distribution of the ϕ_P values from the terminal pulses (i.e., terminal phase) from all entrained trials ($M = 63.8\%, SD = 10.4\%$) was centered about those at which subjects could gain the most mechanical benefit from the exoskeleton robot ($M = 65.1\%, SD = 1.57\%$).

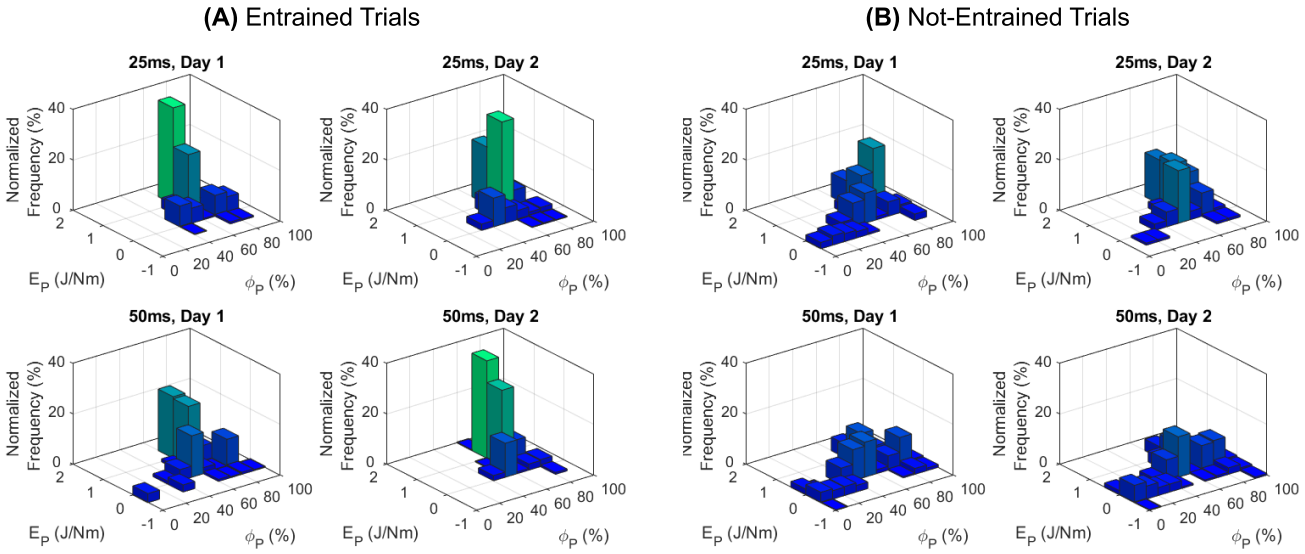

Fig. 5. Histograms of pulse phase (ϕ_P) and mean normalized terminal work done by the robot (E_P) from the last 10 pulses (i.e., terminal pulses) of all **(A)** entrained and **(B)** not-entrained trials in each experimental condition. Color indicates normalized frequency (as does the z-axis); Greener bars denote higher occurrences of a particular combination of ϕ_P and E_P values.

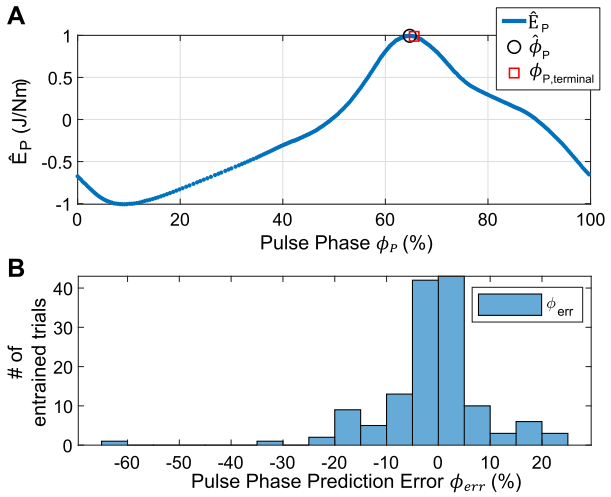

Fig. 6. **(A)** Predicted normalized pulse mechanical energy $\hat{E}_P(\phi_P)$ as a function of pulse phase (continuous line) in a representative trial (group-25ms, day 1, subject 1, trial 1), with predicted locking phase $\hat{\phi}_P$ (black circle) and actual $\phi_{P,terminal}$ (red square). **(B)** Histogram of prediction error ($\phi_{err} = \hat{\phi}_P - \phi_{P,terminal}$) for all entrained trials.

A representative trial exemplifies the similarity between the actual $\phi_{P,terminal}$ and the predicted phase for maximal work done by the robot $\hat{\phi}_P$ (Fig. 6A). The distribution of the error between predicted and actual locking phase ($\phi_{err} = \hat{\phi}_P - \phi_{P,terminal}$) (Fig. 6B) for all entrained trials was centered around zero ($M = -1.3\%, SD = 10.2\%$). These results indicate a close relationship between the converged phase and positive mechanical work done by the robot confirming **hypothesis 4**.

E. Stride Period

Fig. 7 presents how the period deviation of entrained trials and not-entrained trials varied in each condition. In all entrained trials, stride duration adapted to match the torque pulse period, resulting in a mean period deviation close to zero. Upon removal of the robotic intervention, stride durations slowly returned to their pre-perturbation values. Conversely, stride duration did not converge to the torque pulse period in not-entrained trials. T-tests indicated that in each condition, the mean period deviation was not significantly different from zero during entrained trials (group-25ms × day1: $p = 0.51$, group-25ms × day 2: $p = 0.77$, group-50ms × day1: $p = 0.61$, group-50ms × day2: $p = 0.11$), but was significantly different from zero during not-entrained trials (group-25ms × day1: $p < 0.001$, group-25ms × day 2: $p < 0.001$, group-50ms × day1: $p < 0.001$, group-50ms × day2: $p < 0.001$). There was a constant offset in period deviation for not-entrained trials. While this offset was smaller on day 2 of not-entrained trials, in particular of group-25ms, it was larger than that of entrained trials.

IV. Discussion

A. Summary of Results

This study characterized unimpaired human subjects' responses to periodic torque pulses applied about the hip joints during overground walking.

We observed that human subjects entrained their gait to the periodic mechanical torque pulses applied by a hip exoskeleton robot. During this process, subjects synchronized their stride duration to match that of the external mechanical perturbation (Fig. 7). For all groups, by the end of entrained trials, pulse phase converged to a unimodal distribution centered around 63-65% (Fig. 3 and Fig. 4). Further analysis revealed that entrainment occurred such that the mechanical energy flow from the robot to the wearer was maximized (Figs. 5 and 6).

Gait entrainment was observed more often when the pulse period was closer to subjects' preferred stride duration, and

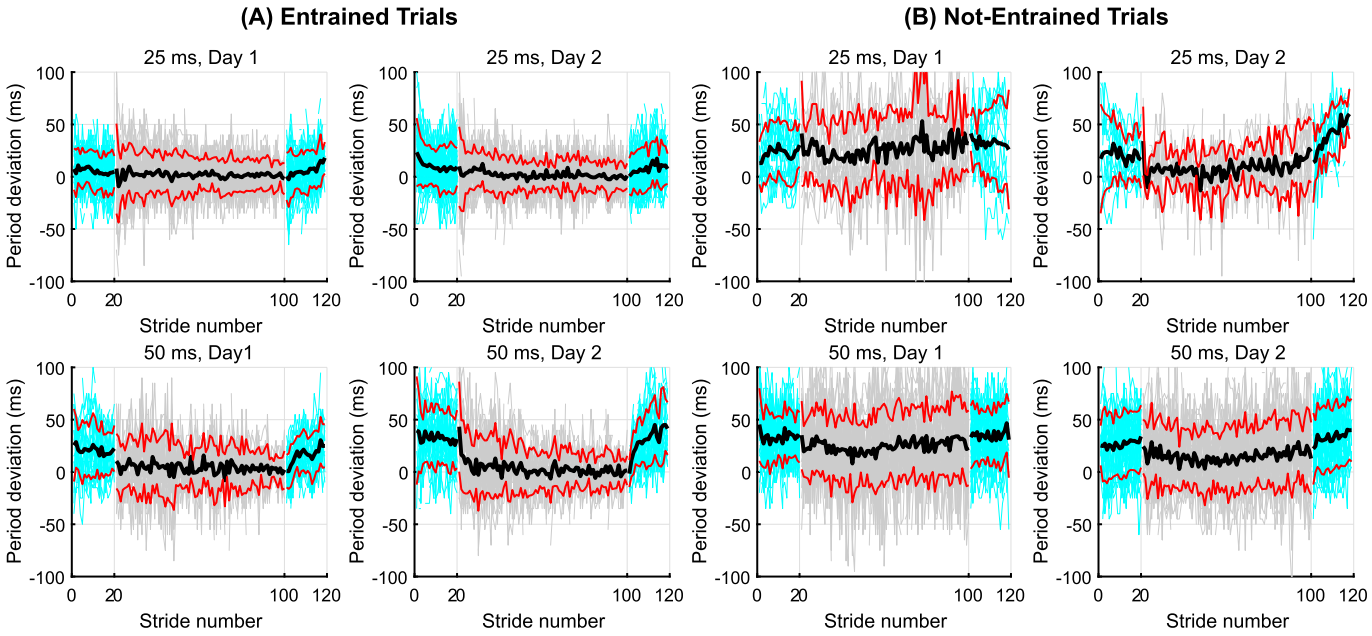

Fig. 7. Period deviation vs. stride number of **A** entrained trials and **B** not-entrained trials. Pre-pulse strides and post-pulse strides are distinguished (cyan). The means and standard deviations of trials for each condition are presented as black, thick lines and red, thin lines, respectively. In computing means and standard deviations for each stride number, outliers were omitted using MATLAB function `rmoutliers` with its default setting. 1142 out of 28,800 total strides (4%) were deemed outliers.

this difference was statistically significant ($p = 0.015$). However, there was no statistical difference between the two days of experiments ($p = 0.55$), suggesting that longer training periods might be required to elicit further changes in neuro-motor behavior or that the effect size of day was too small to detect with the number of subjects included in this study.

B. Limitation: Robot-Embedded Measurements

There are trade-offs between tightly-controlled lab experiments and experiments in real-world conditions. For example, walking overground enables a study of natural human behaviors in more ecological contexts, but the ability to measure human behavior is limited. On the other hand, walking on a treadmill in a lab enables reliable collection of various data (e.g., ground reaction forces using force plates or whole-body kinematics using a motion capture system). However, walking on a treadmill is mechanically different from walking overground. For instance, the treadmill belt speed changes periodically depending on the gait phase, and may require motor adaptation to a dynamic environment [45]. The goal of this study was to investigate entrainment in real-world conditions, despite the associated limitations.

Entrainment was assessed based on robot-embedded joint position measurements. Because the exoskeleton robot did not perfectly conform to each individual, the hip joint angles measured by the robot-embedded encoders may have differed from the true human joint angles. The robot actuators transmitted power and/or torque through a thigh frame and belt assembly that was tightly coupled to the human subjects. However, torque transmission may have been imperfect for a myriad of reasons (e.g., friction in the actuator, elasticity in human tissue or the thigh frame, and relative motion between the exoskeleton robot and the wearer). The difference between torque estimated from on-board sensors and external force-sensitive resistor (FSR) sensors was presented in [46]. Nonetheless, our conclusion that periodic torque pulses at the hip joints induced gait entrainment is still valid because it relies on the trend of behavior rather than exact values. Inaccurate kinematic measurement and inaccurate torque application cannot dismiss our results.

Measurements based on whole-body kinematics (e.g., stride length), or stride segmentation based on external sensors (e.g., foot-mounted sensors) would be useful to confirm and further illuminate our results. In addition, direct measurements of muscle activity (e.g., surface electromyography, sEMG) would be useful to further identify neuro-muscular mechanisms associated with gait entrainment. Measurements of metabolic cost would also add useful information to track consequential changes in locomotion economy following adaptation.

C. Gait Entrainment to Mechanical Perturbations

Periodic torque pulses applied by a hip exoskeleton evoked gait entrainment, accompanied by convergence of pulse phase to a constant value across all conditions. Entrainment occurred more often when the period of perturbation was closer to subjects' natural stride duration. The results are consistent with previous studies that showed entrainment to mechanical perturbations [11], [13], [19]–[21], [47]. While a direct, within-subject comparison of the basin of entrainment for ankle versus hip torque is still needed, the present results suggest that the basin of entrainment is smaller with a hip exoskeleton than with an ankle exoskeleton [11], [13], [47]. For instance,

the percentage of trials entrained to pulse periods 50ms shorter was higher for ankle perturbations (92% of overground trials in [11]) compared to hip perturbations (day1: 39%, 25 out of 64 trials; day2: 45%, 29 out of 64 trials). Assessment of this difference, and identification of the underlying cause, remain areas for future work.

While entrainment itself does not enforce convergence to a particular constant phase, subjects entrained their gait to maximize the work done by the hip exoskeleton robot, as illustrated in Fig. 5. This result is consistent with previous studies with different mechanical interventions, in which individuals adapted to leverage positive power from the devices [48], aligning the timing of robotic torques from an ankle exoskeleton with ankle propulsion [11], [13], [33]. Subjects tended to get the most mechanical assistance during the gait phase when the ankle does the most positive work [49].

Adapting gait to maximize mechanical energy supply from the hip exoskeleton robot has biomechanical advantages. The hip joints produce 40 - 45% of positive power during walking, and this is mostly done during the initial- and mid-swing phases [36]. To get the swing leg out in front requires substantial effort and power, which is influenced by hip torque. The converged pulse phase (63 - 65%) roughly corresponds to when the left leg is extending (from maximum flexion) and the right leg is flexing (See Fig.2A). At this phase the robot drove the legs apart, as it always applied flexion torque pulses on the right and extension on the left, providing assistance to swing the right leg forward. Moreover, this phase also approximately coincides with activity bursts of the major hip flexor muscles of the right leg and hip extensor muscles of the left leg [36]. Additional sEMG measurements would be useful to confirm this explanation. Assuming a major limitation to walking speed is the effort required to get the swing leg out in front, assisting that action may provide some useful therapeutic effect (e.g. for stroke survivors with hemiparesis).

D. Gait Entrainment: Neural or Mechanical?

Does gait entrainment involve any central neural process, or was it purely due to peripheral neuro-mechanics? The potential bio-mechanical benefits discussed in the previous section seem to suggest that biomechanical mechanisms at least played a significant role. In fact, a previous modeling study suggested that gait entrainment may not require any supra-spinal mechanisms [26]. However, that model could not reproduce some experimental results (e.g., entrainment to periodic perturbations slower than preferred walking period [11], [50]), suggesting that some higher-level neural contribution may be required. Indeed, it is hard to dismiss the role of supra-spinal control in gait entrainment.

The intervention in this study was designed to either drive the legs apart or pull them together, depending on the phase at which the pulse occurred. Since the torque pulse period was similar to the stride duration not the step duration, this intervention influenced inter-leg coordination, breaking symmetry, which might be detected by the CNS as an error to be corrected [51]. Mechanical perturbations affecting inter-leg coordination have been shown to evoke locomotor adaptation, e.g., split-belt treadmill walking [51] and many other studies involving unilateral perturbation [52]–[54]. Conversely, our companion study [55] showed that an intervention that did not affect symmetry did not evoke motor adaptation.

Moreover, the timing of locomotor patterns is thought to be mediated at the spinal level (e.g., central pattern generators) but under supraspinal control (e.g., motor cortex, via brainstem centers) and afferent sensory feedback [56]–[59]. While auditory signals cannot directly influence inter-leg coordination, substantial studies have shown that the rhythmic adaptation observed in auditory-motor synchronization involves central neural mechanisms (e.g. cortical areas, basal ganglia and the cerebellum) [18]. There is also evidence that neuro-motor adaptation to a mechanical perturbation was predominantly due to descending drive from supra-spinal levels [60]. For example, an intact cerebellum and motor cortex appear to be critical for motor adaptation [61].

In sum, it seems reasonable to suggest that both high-level (supra-spinal) control and low-level peripheral neuromechanical structures contributed to the observed gait entrainment to mechanical perturbation at the hip joints.

E. A Nonlinear Limit-Cycle Oscillator as a Descriptive Model of Human Walking

When exposed to external periodic forcing, a nonlinear limit cycle oscillator is entrained and synchronizes its frequency with that of the stimulus [62]. This synchronization only occurs when the frequency and strength of the stimuli are in a finite region called the basin of entrainment[1]; outside this region in parameter space, entrainment does not occur.

The experiments reported here were designed based on a working hypothesis that a nonlinear, stable limit cycle oscillator is a reasonable descriptive model of human walking. The experimental observations of this study can be summarized by two characteristics: phase-locking to a unimodal phase distribution; and a finite basin of entrainment (more entrainment in group-25ms than in group-50ms). Inevitable noise in biological systems was also observed, e.g., in stride durations or pulse phase distributions. Despite the unquestionable complexity of the human neuromotor system, there is considerable practical value to describing human walking with an exoskeleton robot by a simplified mathematical model: a nonlinear limit-cycle oscillator with periodic forcing, subject to the presence of stochasticity. Note that a linear model (e.g. a second-order mass-spring-damper system) cannot exhibit a finite basin of entrainment. Despite the evident power of linear analysis, some phenomena require nonlinearity. Stochasticity is also required, though deterministic chaos may not be necessary [63].

This simple theoretical model provides useful insights to predict and interpret complicated experimental observations. First, the finite basin of entrainment is determined by two parameters: the period of perturbation and the coupling strength. From this point of view, it is natural to observe less entrainment in group-50ms than in group-25ms. When the parameters

[1]It is also said that the system exhibits the *Arnold's tongue* structure, due to the shape of the basin of entrainment.

are outside the basin of entrainment, entrainment will not occur and the pulse phase will drift. However, when the parameters are close to the boundary, the pulse phase will drift slowly when it is near the converged phase (critical slowing [64]). In that case, stochasticity may 'push' the system into the basin of entrainment. We believe this is what we observed in some trials in Fig. 3.

Second, this simple theoretical model might potentially be useful to quantify individuals with a small number of parameters. For example, the model presented in [62] only requires three parameters: the convergence rate of the limit cycle (this may be a characteristic of individual subjects), the relative frequency between the stimulus (pulse period T_p) and the oscillator (subjects' preferred stride duration T_o), and the coupling strength (which may be related to pulse magnitude τ_m or pulse duration T_d or both). A model of this kind may serve to customize treatment protocols to individual patients.

F. Gait Entrainment: Clinical Implications

Mechanical gait entrainment may serve as a novel *permissive* locomotor rehabilitation therapy that does not disrupt the limit-cycle behavior underlying locomotion. Similar to the auditory gait entrainment which has shown promising therapeutic effects [17], mechanically entraining gait to increase cadence may result in increased walking speed [15], [65] or stride length [17], which might be important functional outcomes for post-stroke survivors [66], [67]. Moreover, walking in recovering stroke patients (and in some healthy elders) looks a lot like a sporadic slow sequence of individual steps. Mechanical entrainment may promote more natural (rhythmic) action and hence be beneficial as demonstrated in [14].

To maximize the potential therapeutic effects of mechanical gait entrainment, different torque pulse profiles (including continuous rhythmic torque patterns) and performance-based protocols for gradual improvement [14], [47], [68] should be investigated. To understand underlying neuro-mechanical mechanisms of entrainment, a competent model would be insightful [69]. Once the most effective method has been established, studies with patient populations should follow to evaluate whether neuromotor adaptation in healthy subjects translates to neuro-recovery in clinical settings. These matters are left for future studies.

Appendix I
Off-Line Stride Segmentation

For each pulse trial, the time-series of left hip angle θ_L was post-processed to detect the peaks using a peak detection algorithm (MATLAB `findpeaks`). The indices of the peaks were stored $i_{pk} \in \mathcal{I}_{PK}$ and served as an initial seed for optimization for stride segmentation (Fig. 8A). The indices of the onset and offset pair of each torque pulse τ_L were stored as tuples: $(i_{on}, i_{off}) \in \mathcal{I}_{ON-OFF}$. If a peak index i_{pk} was within any pair of indices $[i_{on}, i_{off}]$, the corresponding stride segmentation was deemed affected by the torque pulse. Those peaks were removed from $\mathcal{I}_{PK}$ and stored as decision variables to be updated, $\mathcal{I}_{DV}$ (See Algorithm 1).

Algorithm 1 Off-Line Stride Segmentation Initialization

Given left hip angle peak indices $\mathcal{I}_{PK}$, torque pulse onset-offset index tuples $\mathcal{I}_{ON-OFF}$
Initialize decision variable $\mathcal{I}_{DV}$
for $i_{pk} \in \mathcal{I}_{PK}$ **do**
  if $\exists (i_{on}, i_{off}) \in \mathcal{I}_{ON-OFF}$ s.t. $i_{pk} \in [i_{on}, i_{off}]$ **then**
    $i_{dv} \leftarrow i_{pk}$
    Append $\mathcal{I}_{DV}$ with i_{dv}
    Remove i_{pk} from $\mathcal{I}_{PK}$
  end if
end for

Algorithm 2 Inter-Stride Variability

procedure INTER-STRIDE VAR($\theta_L, \theta_R, \mathcal{I}_{PK}, \mathcal{I}_{DV}, N$)
  Initialize $V \leftarrow 0$
  Initialize stride segments $\mathcal{S}$
  Sort $\mathcal{I}_S = \mathcal{I}_{PK} \cup \mathcal{I}_{DV}$ in ascending order
  for s-th index $i_s \in \mathcal{I}_S$ **do**
    $\boldsymbol{\theta}_L^{(s)} \leftarrow (\theta_L[i_s], \theta_L[i_s+1], \cdots, \theta_L[i_{s+1}])$
    $\boldsymbol{\theta}_R^{(s)} \leftarrow (\theta_R[i_s], \theta_R[i_s+1], \cdots, \theta_R[i_{s+1}])$
    $\boldsymbol{\theta}_L^{(s)} \leftarrow \texttt{interp1}((i_s, \cdots, i_{s+1}), \boldsymbol{\theta}_L^{(s)}, (1, \cdots, N))$
    $\boldsymbol{\theta}_R^{(s)} \leftarrow \texttt{interp1}((i_s, \cdots, i_{s+1}), \boldsymbol{\theta}_R^{(s)}, (1, \cdots, N))$
    Store $\boldsymbol{\theta}_L^{(s)}, \boldsymbol{\theta}_R^{(s)}$ in $\mathcal{S}$
  end for
  Compute ensemble average: $\bar{\boldsymbol{\theta}}_L$ and $\bar{\boldsymbol{\theta}}_R$
  for $\boldsymbol{\theta}_L^{(s)}, \boldsymbol{\theta}_R^{(s)} \in \mathcal{S}$ **do**
    $V \leftarrow V + \|\boldsymbol{\theta}_L^{(s)} - \bar{\boldsymbol{\theta}}_L\|^2 + \|\boldsymbol{\theta}_R^{(s)} - \bar{\boldsymbol{\theta}}_R\|^2$
  end for
  return V
end procedure

Assuming human subjects exhibited similarity across different strides within each trial, the decision variables were updated so as to minimize inter-stride variability V. To compute inter-stride variability V, the time-series of left θ_L and right θ_R hip angle were first segmented using $\mathcal{I}_{PK} \cup \mathcal{I}_{DV}$. Each stride segment was interpolated and time-normalized as a length N vector (MATLAB `interp1`). The inter-stride variability was calculated as the sum of squared errors of each stride and the ensemble average; see Algorithm 2.

In this work, the genetic algorithm (MATLAB function `ga`) was used to find the integer-valued decision variables $\mathcal{I}_{DV}$ that globally minimized V. Other methods may be developed for computational efficiency. To avoid over-correction, each of the corrected peak indices (i_{dv}) was bounded in time by $\pm T_d$ ($= \pm$ 200 ms) from its initial value (i_{pk}). The optimal stride segments $\mathcal{S}$ were used to calculate dependent measures in this study.

The effect of the developed stride segmentation algorithm is clearly demonstrated in Fig. 8. When motion artifacts were significant as in this study (due to relative motion between the exoskeleton robot and the wearers), this method outperformed the näive peak detection algorithm to segment strides from long time-series data (e.g., MATLAB `findpeaks`). Of course, using external sensors such as a motion capture

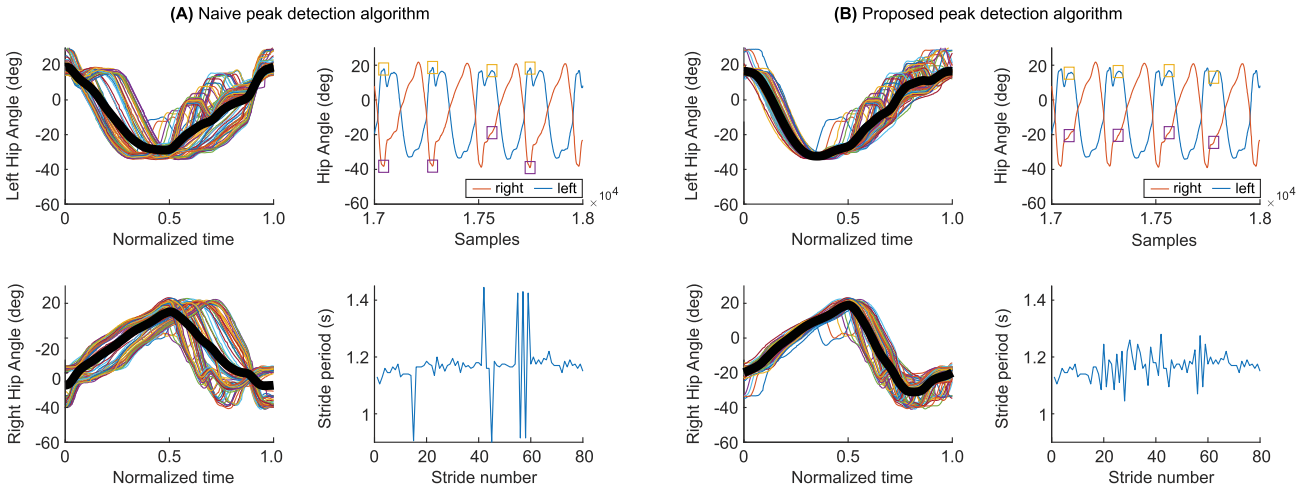

Fig. 8. Stride segmentation using naive peak detection algorithm (A) and using the improved algorithm (B). Each segment of the data between squares (top, right of each panel) corresponds to a stride.

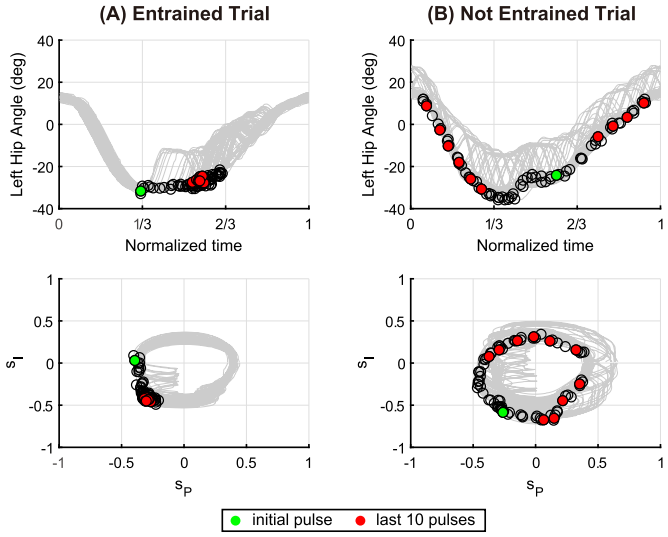

Fig. 9. Representative entrained trial (A) and not entrained trial (B). Top: Hip angle (positive: extension; negative: flexion) vs. normalized time. All 80 strides of the representative trial. Bottom: trajectory of s_P vs. s_I of all strides on the phase plane. Black circles indicate the onsets of torque pulses. Green dot indicates the initial pulse. Red dots indicate the onsets of ten terminal pulses.

system or a force plate to detect gait events would be more accurate, but may not be compatible with human studies outside the lab.

Appendix II
Phase Estimation Algorithm

The phase estimation algorithm was adopted from [25], [43], [44]. For the s-th stride $\boldsymbol{\theta}_L^{(s)} \in \mathcal{S}$ from Appendix I, the angle and its integral were shifted and scaled to obtain two signals $\boldsymbol{s}_P^{(s)}$ and $\boldsymbol{s}_I^{(s)}$.

$$\boldsymbol{s}_P^{(s)} = \boldsymbol{\theta}_L^{(s)} - \frac{1}{N}\sum_{i=1}^{N}\boldsymbol{\theta}_L^{(s)}[i] \tag{2}$$

$$\hat{\boldsymbol{s}}_I^{(s)}[k] = \sum_{i=1}^{k}\boldsymbol{s}_P^{(s)}[i] \tag{3}$$

$$g^{(s)} = \frac{\max \boldsymbol{s}_P^{(s)} - \min \boldsymbol{s}_P^{(s)}}{\max \hat{\boldsymbol{s}}_I^{(s)} - \min \hat{\boldsymbol{s}}_I^{(s)}} \tag{4}$$

$$\boldsymbol{s}_I^{(s)} = g\hat{\boldsymbol{s}}_I^{(s)} \tag{5}$$

The two signals $\boldsymbol{s}_P^{(s)}$ and $\boldsymbol{s}_I^{(s)}$ construct a closed orbit on the phase plane. The phase of each data point for each stride was computed as the angle of the data point on the phase plane as shown in Fig. 9.

$$\boldsymbol{\phi}^{(s)}[i] = \frac{1}{2\pi}atan\left(\frac{\boldsymbol{s}_I^{(s)}[i]}{\boldsymbol{s}_P^{(s)}[i]}\right) \in [0, 1]. \tag{6}$$

References

[1] H. S. Kaye, T. Kang, and M. P. LaPlante, *Mobility Device Use in the United States* (Disability Statistics Report 14), vol. 14. Washington, DC, USA: Department of Education, National Institute on Disability and Rehabilitation Research, 2000.

[2] United Nations, Department of Economic and Social Affairs, Population Division. (2017). *World Population Prospects: The 2017 Revision, Key Findings and Advance Tables ESA/P/WP/248*. [Online]. Available: https://population.un.org/wpp/Publications/Files/WPP2017_KeyFindings.pdf

[3] H. S. Jørgensen, H. Nakayama, H. O. Raaschou, and T. S. Olsen, "Recovery of walking function in stroke patients: The Copenhagen stroke study," *Arch. Phys. Med. Rehabil.*, vol. 76, no. 1, pp. 27–32, Jan. 1995.

[4] V. L. Feigin, B. Norrving, and G. A. Mensah, "Global burden of stroke," *Circulat. Res.*, vol. 120, no. 3, pp. 439–448, 2017.

[5] W. H. Chang and Y.-H. Kim, "Robot-assisted therapy in stroke rehabilitation," *J. Stroke*, vol. 15, no. 3, pp. 174–181, 2013.

[6] J. Mehrholz, B. Elsner, C. Werner, J. Kugler, and M. Pohl, "Electromechanical-assisted training for walking after stroke," *Stroke*, vol. 44, no. 10, pp. 1–206, Oct. 2013. [Online]. Available: https://www.cochranelibrary.com/cdsr/doi/10.1002/14651858.CD006185.pub5/full

[7] J. Hidler *et al.*, "Multicenter randomized clinical trial evaluating the effectiveness of the lokomat in subacute stroke," *Neurorehabil. Neural Repair*, vol. 23, no. 1, pp. 5–13, Jan. 2009.

[8] D. R. Louie and J. J. Eng, "Powered robotic exoskeletons in post-stroke rehabilitation of gait: A scoping review," *J. NeuroEng. Rehabil.*, vol. 13, no. 1, pp. 1–10, Dec. 2016.

[9] F. Molteni *et al.*, "Gait recovery with an overground powered exoskeleton: A randomized controlled trial on subacute stroke subjects," *Brain Sci.*, vol. 11, no. 1, p. 104, Jan. 2021.

[10] A. Jayaraman *et al.*, "Stride management assist exoskeleton vs functional gait training in stroke: A randomized trial," *Neurology*, vol. 92, no. 3, pp. e263–e273, Jan. 2019.

[11] J. Ochoa, D. Sternad, and N. Hogan, "Treadmill vs. Overground walking: Different response to physical interaction," *J. Neurophysiol.*, vol. 118, no. 4, pp. 2089–2102, Oct. 2017.

[12] M. F. Bruni, C. Melegari, M. C. De Cola, A. Bramanti, P. Bramanti, and R. S. Calabrè, "What does best evidence tell us about robotic gait rehabilitation in stroke patients: A systematic review and meta-analysis," *J. Clin. Neurosci.*, vol. 48, pp. 11–17, Feb. 2018.

[13] J. Ahn and N. Hogan, "Walking is not like reaching: Evidence from periodic mechanical perturbations," *PLoS ONE*, vol. 7, no. 3, Mar. 2012, Art. no. e31767.

[14] J. Ahn *et al.*, "Feasibility of entrainment with ankle mechanical perturbation to treat locomotor deficit of neurologically impaired patients," in *Proc. Annu. Int. Conf. Eng. Med. Biol. Soc.*, 2011, pp. 7474–7477.

[15] L.-A. Leow, T. Parrott, and J. A. Grahn, "Individual differences in beat perception affect gait responses to low and high-groove music," *Frontiers Hum. Neurosci.*, vol. 8, p. 811, Oct. 2014.

[16] E. A. Ready, L. M. McGarry, C. Rinchon, J. D. Holmes, and J. A. Grahn, "Beat perception ability and instructions to synchronize influence gait when walking to music-based auditory cues," *Gait Posture*, vol. 68, pp. 555–561, Feb. 2019.

[17] V. C. De Cock *et al.*, "Rhythmic abilities and musical training in Parkinson's disease: Do they help?" *NPJ Parkinson's Disease*, vol. 4, no. 1, pp. 1–8, 2018.

[18] L. Damm, D. Varoqui, V. C. De Cock, S. Dalla Bella, and B. Bardy, "Why do we move to the beat? A multi-scale approach, from physical principles to brain dynamics," *Neurosci. Biobehav. Rev.*, vol. 112, pp. 553–584, 2020.

[19] E. Tackett and J. Nessler, "Sensorimotor synchronization during gait is altered by the addition of variability to an external cue," *Hum. Movement Sci.*, vol. 71, Jun. 2020, Art. no. 102626.

[20] J. A. Nessler, S. Heredia, J. Bélair, and J. Milton, "Walking on a vertically oscillating treadmill: Phase synchronization and gait kinematics," *PLoS ONE*, vol. 12, no. 1, Jan. 2017, Art. no. e0169924.

[21] R. T. Schroeder, J. L. Croft, and J. E. A. Bertram, "Evaluating the energetics of entrainment in a human–machine coupled oscillator system," *Sci. Rep.*, vol. 11, p. 15804, 2021. [Online]. Available: https://www.nature.com/articles/s41598-021-95047-x, doi: 10.1038/s41598-021-95047-x.

[22] K. Nishimura, E. Martinez, A. Loeza, J. Parker, and S.-J. Kim, "Effects of periodic sensory perturbations during electrical stimulation on gait cycle period," *PLoS ONE*, vol. 13, no. 12, Dec. 2018, Art. no. e0209781.

[23] J. E. Thorp and P. G. Adamczyk, "Mechanisms of gait phase entrainment in healthy subjects during rhythmic electrical stimulation of the medial gastrocnemius," *PLoS ONE*, vol. 15, no. 10, Oct. 2020, Art. no. e0241339.

[24] J. Lee, D. Goetz, M. E. Huber, and N. Hogan, "Feasibility of gait entrainment to hip mechanical perturbation for locomotor rehabilitation," in *Proc. IEEE/RSJ Int. Conf. Intell. Robot. Syst. (IROS)*, Feb. 2019, pp. 7343–7348.

[25] D. J. Villarreal, H. A. Poonawala, and R. D. Gregg, "A robust parameterization of human gait patterns across phase-shifting perturbations," *IEEE Trans. Neural Syst. Rehabil. Eng.*, vol. 25, no. 3, pp. 265–278, Mar. 2017.

[26] J. Ahn and N. Hogan, "A simple state-determined model reproduces entrainment and phase-locking of human walking," *PLoS ONE*, vol. 7, no. 11, Nov. 2012, Art. no. e47963.

[27] K. Seo, J. Lee, Y. Lee, T. Ha, and Y. Shim, "Fully autonomous hip exoskeleton saves metabolic cost of walking," in *Proc. Int. Conf. Robot. Autom. (ICRA)*, 2016, pp. 4628–4635.

[28] J. Lee, K. Seo, B. Lim, J. Jang, K. Kim, and H. Choi, "Effects of assistance timing on metabolic cost, assistance power, and gait parameters for a hip-type exoskeleton," in *Proc. Int. Conf. Rehabil. Robot. (ICORR)*, 2017, pp. 498–504.

[29] Y. Lee *et al.*, "A flexible exoskeleton for hip assistance," in *Proc. Int. Conf. Intell. Robot. Syst. (IROS)*, 2017, pp. 1058–1063.

[30] B. Lim *et al.*, "Delayed output feedback control for gait assistance with a robotic hip exoskeleton," *IEEE Trans. Robot.*, vol. 35, no. 4, pp. 1055–1062, Aug. 2019.

[31] B. T. Quinlivan *et al.*, "Assistance magnitude versus metabolic cost reductions for a tethered multiarticular soft exosuit," *Sci. Robot.*, vol. 2, no. 2, p. 4416, Jan. 2017.

[32] J. M. Caputo and S. H. Collins, "An experimental robotic testbed for accelerated development of ankle prostheses," in *Proc. Int. Conf. Robot. Autom.*, 2013, pp. 2645–2650.

[33] K. E. Gordon and D. P. Ferris, "Learning to walk with a robotic ankle exoskeleton," *J. Biomech.*, vol. 40, no. 12, pp. 2636–2644, 2007.

[34] J. Zhang *et al.*, "Human-in-the-loop optimization of exoskeleton assistance during walking," *Science*, vol. 356, no. 6344, pp. 1280–1284, Jun. 2017.

[35] K. C. Moisio, D. R. Sumner, S. Shott, and D. E. Hurwitz, "Normalization of joint moments during gait: A comparison of two techniques," *J. Biomech.*, vol. 36, no. 4, pp. 599–603, Apr. 2003.

[36] J. Perry and J. Burnfield, *Gait Analysis: Normal Pathological Function*. West Deptford, NJ, USA: Slack, 2010.

[37] B. Boashash, "Estimating and interpreting the instantaneous frequency of a signal. I. Fundamentals," *Proc. IEEE*, vol. 80, no. 4, pp. 520–538, Apr. 1992.

[38] M. G. Rosenblum, A. S. Pikovsky, and J. Kurths, "Phase synchronization in driven and coupled chaotic oscillators," *IEEE Trans. Circuits Syst. I, Fundam. Theory Appl.*, vol. 44, no. 10, pp. 874–881, Oct. 1997.

[39] S. Revzen and J. M. Guckenheimer, "Estimating the phase of synchronized oscillators," *Phys. Rev. E, Stat. Phys. Plasmas Fluids Relat. Interdiscip. Top.*, vol. 78, no. 5, Nov. 2008, Art. no. 051907.

[40] S. Revzen, S. A. Burden, T. Y. Moore, J.-M. Mongeau, and R. J. Full, "Instantaneous kinematic phase reflects neuromechanical response to lateral perturbations of running cockroaches," *Biol. Cybern.*, vol. 107, no. 2, pp. 179–200, Apr. 2013.

[41] E. R. Westervelt, J. W. Grizzle, C. Chevallereau, J. H. Choi, and B. Morris, *Feedback Control of Dynamic Bipedal Robot Locomotion*. Boca Raton, FL, USA: CRC Press, 2018.

[42] D. J. Villarreal and R. D. Gregg, "A survey of phase variable candidates of human locomotion," in *Proc. 36th Annu. Int. Conf. Eng. Med. Biol. Soc.*, 2014, pp. 4017–4021.

[43] D. Quintero, D. J. Villarreal, D. J. Lambert, S. Kapp, and R. D. Gregg, "Continuous-phase control of a powered knee–ankle prosthesis: Amputee experiments across speeds and inclines," *IEEE Trans. Robot.*, vol. 34, no. 3, pp. 686–701, Jun. 2018.

[44] D. J. Villarreal and R. D. Gregg, "Controlling a powered transfemoral prosthetic leg using a unified phase variable," in *Wearable Robotics*. Amsterdam, The Netherlands: Elsevier, 2020, pp. 487–506.

[45] A. Tielke, J. Ahn, and H. Lee, "Non-ideal behavior of a treadmill depends on gait phase, speed, and weight," *Sci. Rep.*, vol. 9, no. 1, pp. 1–12, Dec. 2019.

[46] H. Choi, K. Seo, S. Hyung, Y. Shim, and S.-C. Lim, "Compact hip-force sensor for a gait-assistance exoskeleton system," *Sensors*, vol. 18, no. 2, p. 566, Feb. 2018.

[47] C. Thalman, M. P. Debeurre, and H. Lee, "Entrainment during human locomotion using a soft wearable ankle robot," *IEEE Robot. Autom. Lett.*, vol. 6, no. 3, pp. 4265–4272, Jul. 2021.

[48] M. Bertrand-Charette, J. B. Nielsen, and L. J. Bouyer, "A simple, clinically applicable motor learning protocol to increase push-off during gait: A proof-of-concept," *PLoS ONE*, vol. 16, no. 1, Jan. 2021, Art. no. e0245523.

[49] D. J. Farris and G. S. Sawicki, "The mechanics and energetics of human walking and running: A joint level perspective," *J. Roy. Soc. Interface*, vol. 9, no. 66, pp. 110–118, Jan. 2012.

[50] D. Rigobon, J. Ochoa, and N. Hogan, "Entrainment of ankle-actuated walking model to periodic perturbations via leading leg angle control," *Proc. SPIE Dyn. Syst. Amer. Soc. Mech. Eng.*, vol. 58271, Oct. 2017, Art. no. V001T36A002.

[51] D. S. Reisman, H. J. Block, and A. J. Bastian, "Interlimb coordination during locomotion: What can be adapted and stored?" *J. Neurophysiol.*, vol. 94, no. 4, pp. 2403–2415, 2005.

[52] K. Fortin, A. Blanchette, B. J. McFadyen, and L. J. Bouyer, "Effects of walking in a force field for varying durations on aftereffects and on next day performance," *Exp. Brain Res.*, vol. 199, no. 2, p. 145, 2009.

[53] A. Blanchette, H. Moffet, J.-S. Roy, and L. J. Bouyer, "Effects of repeated walking in a perturbing environment: A 4-day locomotor learning study," *J. Neurophysiol.*, vol. 108, no. 1, pp. 275–284, Jul. 2012.

[54] T. Lam, M. Anderschitz, and V. Dietz, "Contribution of feedback and feedforward strategies to locomotor adaptations," *J. Neurophysiol.*, vol. 95, no. 2, pp. 766–773, Feb. 2006.

[55] J. Lee, M. E. Huber, and N. Hogan, "Applying hip stiffness with an exoskeleton to compensate gait kinematics," *IEEE Trans. Neural Syst. Rehabil. Eng.*, vol. 29, pp. 2645–2654, 2021.

[56] K. Minassian, U. S. Hofstoetter, F. Dzeladini, P. A. Guertin, and A. Ijspeert, "The human central pattern generator for locomotion: Does it exist and contribute to walking?" *Neuroscientist*, vol. 23, no. 6, pp. 649–663, Dec. 2017.

[57] G. Taga, Y. Yamaguchi, and H. Shimizu, "Self-organized control of bipedal locomotion by neural oscillators in unpredictable environment," *Biol. Cybern.*, vol. 65, no. 3, pp. 147–159, Jul. 1991.

[58] P. A. Guertin, "Central pattern generator for locomotion: Anatomical, physiological, and pathophysiological considerations," *Frontiers Neurol.*, vol. 3, p. 183, Oct. 2013.

[59] C. C. Maguire, J. M. Sieben, and R. A. de Bie, "The influence of walking-aids on the plasticity of spinal interneuronal networks, central-pattern-generators and the recovery of gait post-stroke. A literature review and scholarly discussion," *J. Bodywork Movement Therapies*, vol. 21, no. 2, pp. 422–434, Apr. 2017.

[60] P.-C. Kao, C. L. Lewis, and D. P. Ferris, "Short-term locomotor adaptation to a robotic ankle exoskeleton does not alter soleus Hoffmann reflex amplitude," *J. Neuroeng. Rehabil.*, vol. 7, no. 1, pp. 1–8, Dec. 2010.

[61] R. Shadmehr, "Learning to predict and control the physics of our movements," *J. Neurosci.*, vol. 37, no. 7, pp. 1663–1671, 2017.

[62] L. Glass and J. Sun, "Periodic forcing of a limit-cycle oscillator: Fixed points, Arnold tongues, and the global organization of bifurcations," *Phys. Rev. E, Stat. Phys. Plasmas Fluids Relat. Interdiscip. Top.*, vol. 50, no. 6, p. 5077, 1994.

[63] J. Ahn and N. Hogan, "Long-range correlations in stride intervals may emerge from non-chaotic walking dynamics," *PLoS ONE*, vol. 8, no. 9, Sep. 2013, Art. no. e73239.

[64] S. H. Strogatz, *Nonlinear Dynamics and Chaos With Student Solutions Manual: With Applications to Physics, Biology, Chemistry, and Engineering*. Boca Raton, FL, USA: CRC Press, 2018.

[65] D. G. Dotov *et al.*, "The role of interaction and predictability in the spontaneous entrainment of movement," *J. Exp. Psychol. Gen.*, vol. 148, no. 6, p. 1041, 2019.

[66] A. Schmid *et al.*, "Improvements in speed-based gait classifications are meaningful," *Stroke*, vol. 38, no. 7, pp. 2096–2100, Jul. 2007.

[67] K. K. Patterson, W. H. Gage, D. Brooks, S. E. Black, and W. E. McIlroy, "Evaluation of gait symmetry after stroke: A comparison of current methods and recommendations for standardization," *Gait Posture*, vol. 31, no. 2, pp. 241–246, 2010.

[68] H. I. Krebs, J. J. Palazzolo, L. Dipietro, M. Ferraro, J. Krol, K. Rannekleiv, B. T. Volpe, and N. Hogan, "Rehabilitation robotics: Performance-based progressive robot-assisted therapy," *Autonom. Robot.*, vol. 15, no. 1, pp. 7–20, Jul. 2003.

[69] B. Abdikadirova, J. Lee, N. Hogan, and M. Huber, "Muscle-reflex model of human locomotion entrains to mechanical perturbations," in *Proc. Int. Conf. Intell. Robot. Syst. (IROS)*, Sep. 2021, pp. 544–7549.